ELSEVIER

Journal of Nuclear Materials 279 (2000) 351–355

journal of nuclear materials

www.elsevier.nl/locate/jnucmat

Letter to the Editors

Comparison of the chemical erosion of Si, C and SiC under deuterium ion bombardment

M. Balden *, J. Roth

Max-Planck-Institut für Plasmaphysik, EURATOM Association, Postfach 1533, Boltzmannstr. 2, D-85748 Garching bei München, Germany

Received 17 December 1999; accepted 3 March 2000

Abstract

Erosion yields of Si, C and SiC due to D ion impact were determined between 20 and 300 eV up to 1100 K. A temperature dependence of the erosion yield has been observed for Si and C. The temperature of the maximum increases with ion energy from about 350 K for 20 eV to 570 K above 100 eV for Si, which is always about 250 K lower than for graphite. The erosion yields of Si are in general 10 times smaller than those of graphite. Chemical erosion species were observed mass-spectroscopically: silane was found for Si, but not for SiC, where only hydrocarbons were observed. © 2000 Elsevier Science B.V. All rights reserved.

1. Introduction

The use of graphite or CFC material in thermonuclear fusion reactors suffers from the high chemical reactivity of carbon with energetic hydrogen ions (for a review, see [1]). Erosion yields for carbon under deuterium irradiation are of the order of 10^{-2} for ion energies down to a few eV, leading to high erosion rates, plasma dilution, limited compound lifetime and large inventory of tritium in deposited carbon layers. The most recent ITER design [2] attempts to limit the use of carbon material as much as possible, restricting it to surface areas of extreme heat load. Especially, the large wall areas of the main plasma chamber of divertor experiments do not experience large heat load, and alternative materials are considered. The ITER design has chosen Be as the wall material exhibiting no chemical erosion and low hydrogen co-deposition in clean Be layers [3]. However, it can be shown that physical sputtering of Be, a low-Z material with low surface binding energy, shows yields comparable to chemical erosion of graphite, and oxidized Be retains similar amounts of hydrogen isotopes as carbon [4,5].

Alternatives discussed include high-Z materials, such as Mo and W, which are, however, detrimental to plasma performance in high confinement phases [6–8]. Often, high-Z wall materials are only tolerable after wall coating with low-Z (C, B, Be) [6,9] or medium-Z (Si) [10,11] layers. The success of siliconization in ASDEX Upgrade [11,12] suggests the use of SiC/SiC tiles as wall material in the main vessel, Si-doped CFC NS31 as divertor target material [13,14] combined with the conditioning method of siliconization [10]. Erosion studies on SiC/SiC [15–17] have shown the absence of chemical erosion while indications of the formation of volatile silane exist for Si [18,19].

In the present investigation, the erosion yields of Si, C and SiC were compared with special emphasis on chemically eroded species by deuterium ions in the energy range between 20 and 300 eV.

2. Experimental

The experiments were performed at the Garching high current ion source [20]. Mass-analyzed ion beams of D_3^+ were produced with an energy of 3 keV and decelerated to 40 eV by biasing the target without a major

---

* Corresponding author. Tel.: +49-89 3299 1688; fax: +49-89 3299 1212.

E-mail address: martin.balden@ipp.mpg.de (M. Balden).

PII: S0022-3115(00)00032-5

loss in the beam current. Ion fluxes in the order of 10^{19} D/m^2 s were achieved. In special cases, for cross-check, a double deflection technique was used, so the small percentage [21] of not decelerated neutrals could not hit the target [22]. In all the cases, the same yields were found with and without double deflection within the error limits of the experiment [14,22].

The targets could be heated by electron bombardment from the rear up to 1100 K during ion bombardment and the temperature was monitored by infrared pyrometry calibrated against optical pyrometry to ±20 K. The base vacuum was 10^{-6} Pa rising to about 10^{-4} Pa during bombardment consisting predominantly of the hydrogen isotope used, while the residual gas pressure of water vapor and methane was further reduced using liquid N_2-cooled shields around the target.

The total erosion yield was measured in situ using a Mettler 22 vacuum micro-balance with a sensitivity <1 μg. Emitted volatile molecules were monitored during the bombardment using a Balzers QMG 511 quadrupole mass analyzer. The cross-beam ionizer of the QMG 511 was surrounded by a liquid nitrogen-cooled shield to reduce residual gas signals from H_2O. Methane signals were calibrated against weight loss in conditions of dominating chemical erosion (1 keV D, about 850 K) and, therefore, also include contributions from heavier hydrocarbons. Silane signal intensities were roughly quantified assuming that mass loss at 20 eV can only occur through volatile molecule emission.

Targets were made from polished pyrolytic graphite cut parallel to the lattice planes (Union Carbide HPG 99), from highly polished SiC single crystals, and from Si single-crystal wavers cut perpendicular to the [1 1 1] direction. All samples were annealed in vacuum for 10 min at 1100 K prior to the erosion experiments.

3. Results and discussion

3.1. Graphite

Total erosion yields of graphite were investigated in detail and published previously [1,19,20,23–25]. A new set of data in the energy range between 15 and 200 eV was measured and published separately in a study aiming at the understanding of the low-energy low-temperature erosion mechanisms [22]. In the present paper, only data for 20, 100 and 300 eV are used for direct comparison with the data for Si and SiC.

The temperature dependence of the erosion yield of graphite shows typically a pronounced maximum at a temperature (T_{max}) around 850 K for ion energies above 100 eV shifting to somewhat lower temperatures with decreasing energy [22] (Fig. 1). The dominant species emitted for D bombardment are CD_4 molecules and their cracking pattern as detected from residual gas analysis (Figs. 2 and 3). Heavier hydrocarbon molecules, such as C_2D_n, are also emitted especially at low ion energies leading to small signals in the mass range 26–32. No physical sputtering of carbon atoms occurs for ion energies of 20 eV at T_{max} and the whole yield of about 7% must be attributed to hydrocarbon emission.

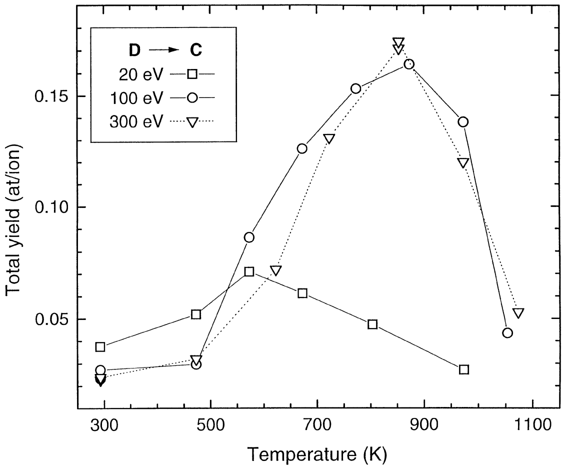

Fig. 1. Temperature dependence of the total erosion yield of pyrolytic graphite (Union Carbide) bombarded with deuterium with an impact energy of 20 eV (squares), 100 eV (circles) and 300 eV (triangles) [22].

3.2. Silicon

Similar to graphite, a pronounced temperature dependence of the total erosion yield is observed also for silicon. Fig. 4 shows the comparison between Si and C for D energies of 20, 100 and 300 eV. The yields of Si at room temperature are comparable to those of graphite for ion impact energies above 100 eV and reach maximum values by a factor of 5 lower than those of graphite. As T_{max} is about 250 K lower for Si than for graphite, i.e., around 550 K, the low-temperature values for Si may even exceed those for graphite.

A drastic decrease of the yields of Si occurs for D energies below 100 eV. The energy dependence of the erosion yields is shown for Si and C at room temperature and 570 K in Fig. 5. The Si yields drop by more than a factor of 10 compared to C to about 0.3% at room temperature for energies around 20 eV. These high yields could be shown for graphite resulting from ion-induced desorption of hydrocarbon radicals [22–25], a process which does not seem to exist for Si, at least not of the same extent. In the case of Si, T_{max} has shifted towards low temperatures with a maximum around 350 K (Fig. 4). This is in very good agreement with the temperature dependence found for thermal hydrogen atoms on Si [18] and indicates that the erosion proceeds

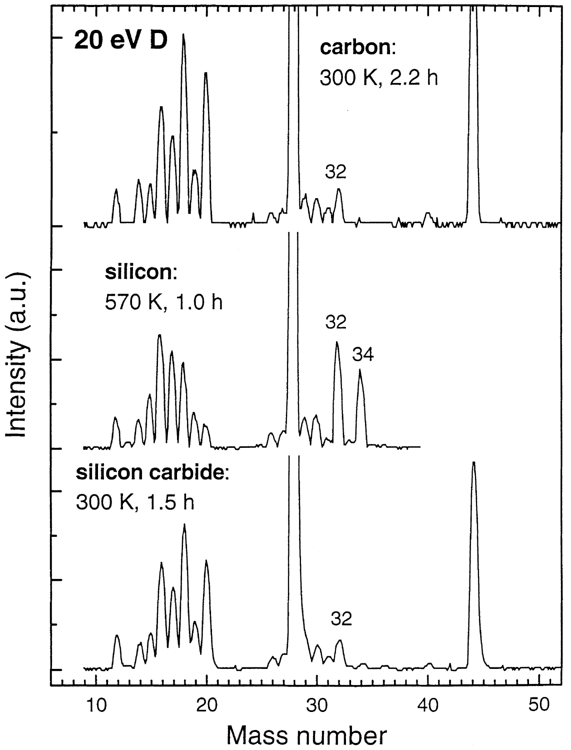

Fig. 2. Mass spectra measured during the D bombardment of C (top), Si (center) and SiC (bottom) with a deuterium impact energy of 20 eV. The target temperature and bombardment duration before recording the mass spectra are labeled.

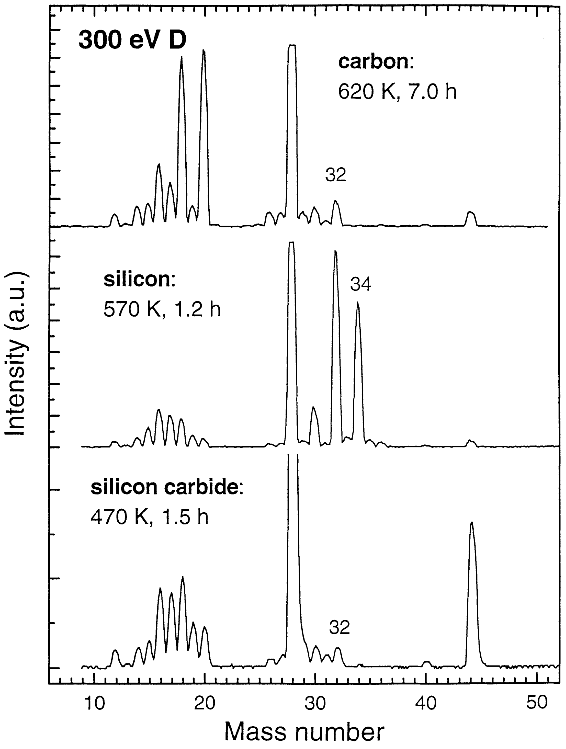

Fig. 3. Mass spectra measured during the D bombardment of C (top), Si (center) and SiC (bottom) with a deuterium impact energy of 300 eV. The target temperature and bombardment duration before recording the mass spectra are labeled.

similar to thermal atomic hydrogen at energies, where no ion-induced erosion or damage processes are possible, i.e., below about 30 eV. In order to avoid any effect of a small fraction of not decelerated neutrals in the ion beam, the low erosion data were cross-checked by measuring the yields with a strongly reduced fraction of neutrals (below 0.3% [22]), shown in Figs. 4 and 5 as crossed symbols. No changes and, therefore, no synergetic effects were observable.

Typical mass spectra are shown in Figs. 2 and 3 for 20 and 300 eV D bombardment at 570 K, which is near the maximum of erosion for 300 eV. The masses 34, 32 and 30 are very prominently observed, typical for the cracking products of deuterated silane, i.e., SiD_3^+, SiD_2^+, and SiD^+. The mass signal at 28 due to CO in the residual atmosphere is dominating in all the presented mass spectra of Figs. 2 and 3, and the correlated signal of CO_2 at mass 44 is visible. Again, at 20 eV the erosion of Si can be assumed to be completely due to molecule/radical emission. If a calibration is done using the mass signal 34 at 20 eV, then the temperature dependence of the mass signal at higher energies follows roughly the weight-loss data if a temperature-independent physical sputtering yield, as obtained from TRIM calculations [20], is taken into account.

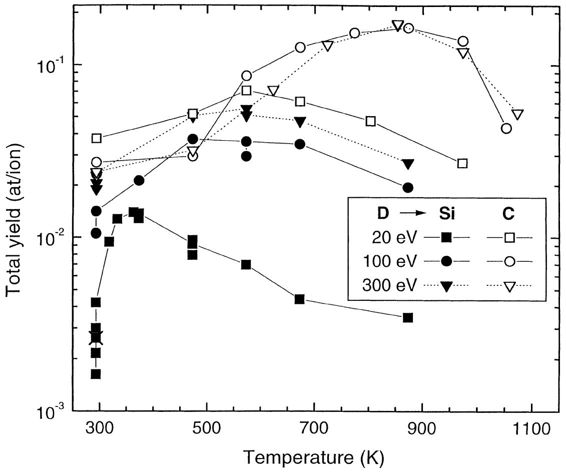

Fig. 4. Temperature dependence of the total erosion yields of Si (solid symbols) and pyrolytic graphite (empty symbols) [22] bombarded with deuterium with an impact energy of 20 eV (squares), 100 eV (circles) and 300 eV (triangles). The crossed data point was measured with reduced amount of not decelerated neutrals (for more details see text).

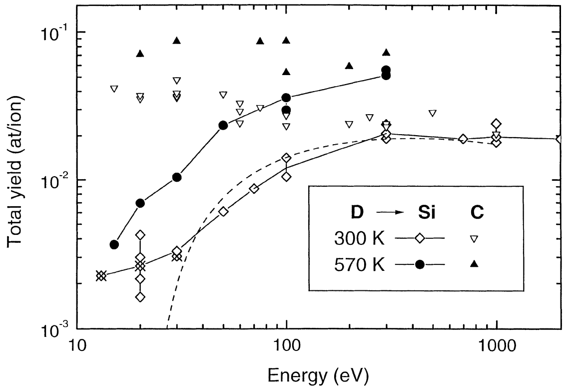

Fig. 5. Energy dependence of the total erosion yields of Si (diamonds, circles) and C (triangles) [22] at room temperature (empty symbols) and 570 K (filled symbols). The crossed data points were measured yields of Si with reduced amount of not decelerated neutrals. The dashed line is the physical sputtering calculated by the revised Bohdansky formula [24–26].

Concerning the mass-spectroscopic signals of silane production, one observation should be mentioned here. In contrast to the methane signals, which show very fast transients with changes in temperature, impact energy or ion flux, the silane signals react very slowly to such changes. Transient times reach values of the order of 30 min. Actually, even closing the vacuum valve between the sputtering chamber and the separately pumped quadrupole leads to a slow decrease of the silane signal over many minutes. The long transients must be attributed to the sticking and desorption of silane to internal surfaces of the vacuum vessel and the quadrupole. Especially due to the liquid nitrogen cooled surfaces in the sputtering chamber and around the quadrupole ionizer, such processes could lead to exceedingly long transients. Collector measurements (like in [22]) give a hint that emitted molecules stick also permanently to surfaces. The calibration of the silane signals by weight loss must be regarded as preliminary. Due to these long transients, the production of silane could have easily been missed in previous investigations.

3.3. Silicon carbide

The chemical erosion mechanism of silicon carbide appears to be much more complicated than that of graphite and silicon. Due to the composition of two elements, surface enrichment processes [16], segregation and diffusion under ion irradiation have to be taken into account and will be discussed in detail in a forthcoming publication [27]. However, in this context, two preliminary findings should be mentioned.

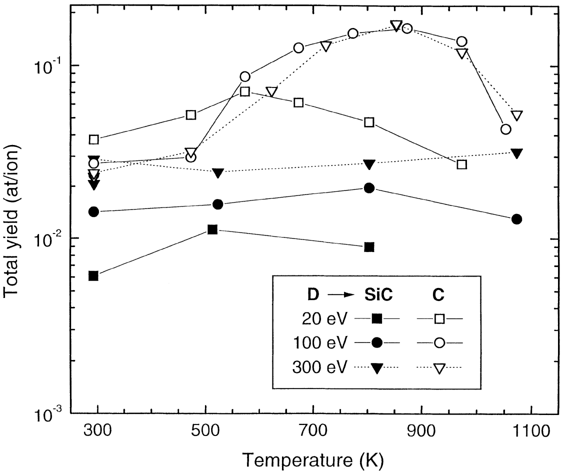

Fig. 6. Temperature dependence of the total erosion yield of crystalline SiC (filled symbols) and pyrolytic graphite (empty symbols) [22] bombarded with deuterium with an impact energy of 20 eV (squares), 100 eV (circles) and 300 eV (triangles).

The temperature dependence of the erosion yield of SiC is very weak, which was often taken as a proof for the absence of chemical erosion [16]. Fig. 6 compares the weight-loss data for SiC to those of graphite as a function of temperature.

On the other hand, yields in the range 0.6–0.8% for energies around 20 eV indicate the presence of a non-collisional erosion process. Actually, the mass signals for methane emission are clearly visible by mass spectroscopy (Figs. 2 and 3), while no indication of silane was observed. The methane signal persists over fluences exceeding the erosion of a surface layer corresponding to many ion ranges and by far the fluences necessary for surface depletion of carbon. Therefore, continuous diffusion processes of carbon in SiC or an additional erosion mechanism of Si have to be assumed. The elucidation of the processes involving ion-induced diffusion, segregation and chemical reactions between D, Si and C need further detailed investigation [27].

4. Conclusion

In comparison with graphite, the chemical erosion of Si under hydrogen irradiation is in general 10 times smaller for temperatures between room temperature and 1100 K and for ion impact energies from 20 to 300 eV. At low ion energies, however, chemical erosion in the form of silane molecules reduces the beneficial effect of the threshold energy for physical sputtering. The temperature dependence of chemical erosion of Si at ion energies of 20 eV shows a maximum around 350 K, very similar to values found earlier for atomic thermal hydrogen [18]. The temperature of the maximum shifts to about 550 K at ion energies above 100 eV, where radiation damage is produced in the Si lattice. Compared to graphite, the temperature of the maximum is always about 250 K lower. The eroded species during bombardment of pure Si were found to be silane molecules, while for SiC the only emitted volatile molecules observed mass-spectroscopically are hydrocarbons, such as methane.

References

[1] E. Vietzke, A.A. Haasz, in: W.O. Hofer, J. Roth (Eds.), Physical Processes in Plasma–Wall Interaction in Nuclear Fusion, Academic Press, NY, 1996.

[2] G. Federici, R.A. Anderl, P. Andrew, J.N. Brooks, R.A. Causey, J.P. Coad, D. Cowgill, P. Doerner, A.A. Haasz, G. Janeschitz, W. Jacob, G.R. Longhorst, R. Nygren, A. Peacock, M.A. Pick, V. Philipps, J. Roth, C.H. Skinner, W.R. Wampler, J. Nucl. Mater. 266–269 (1999) 14.

[3] R.A. Causey, D.S. Walsh, J. Nucl. Mater. 254 (1998) 84.

[4] J.N. Brooks, D. Alman, G. Federici, D.N. Ruzic, D.G. Whyte, J. Nucl. Mater. 266–269 (1999) 58.

[5] M. Mayer, R. Behrisch, H. Plank, J. Roth, G. Dollinger, C.M. Frey, J. Nucl. Mater. 230 (1996) 67.

[6] M.J. May, K.B. Fournier, J.A. Terry, D. Pacella, M. Finkenthal, E.S. Marmar, W.H. Goldstein, Plasma Phys. Control. Fusion 41 (1999) 45.

[7] M. Tokar, J. Rapp, G. Bertschinger, L. Könen, H.R. Koslowski, A. Krämer-Flecken, V. Philipps, U. Samm, B. Unterberg, Nucl. Fusion 37 (1997) 1691.

[8] K. Krieger, H. Maier, R. Neu, J. Nucl. Mater. 266–269 (1999) 207.

[9] M. Mayer, R. Behrisch, P. Andrew, A.T. Peakock, J. Nucl. Mater. 241–243 (1997) 469.

[10] J. Winter, H.G. Esser, G.I. Jackson, L. Könen, A. Messiaen, J. Ongena, V. Philipps, A. Pospieszczyk, U. Samm, B. Schweer, B. Unterberg, Phys. Rev. Lett. 71 (1993) 1549.

[11] V. Rohde, R. Neu, R. Dux, T. Härtl, H. Maier, J. Luthin, H.G. Esser, V. Philipps, in: Proceedings of the 26th EPS Conference on Controlled Fusion and Plasma Physics, vol. 23J, Maastricht, Europhysics Conference Abstracts, 1999, p. 1513.

[12] V. Rohde, H. Maier, K. Krieger, R. Neu, J. Perchermaier, in: Proceedings of the 14th International Conference on Plasma Surface Interactions, Rosenheim, Germany, May 2000, to be published in J. Nucl. Mater. (2001).

[13] C.H. Wu, C. Alessandrini, P. Bonal, A. Caso, H. Grote, R. Moormann, A. Perujo, M. Balden, H. Werle, G. Vieider, Fusion Technol. (special issue, 1996) (1997) 327.

[14] M. Balden, J. Roth, C.H. Wu, J. Nucl. Mater. 258–263 (1998) 740.

[15] H. Plank, R. Schwörer, J. Roth, Surf. Coat. Technol. 83 (1996) 93.

[16] H. Plank, R. Schwörer, J. Roth, Nucl. Instrum. and Meth. B 111 (1996) 63.

[17] J. Roth, H. Plank, R. Schwörer, Phys. Scripta T 64 (1996) 67.

[18] A.P. Webb, S. Veprek, Chem. Phys. Lett. 62 (1979) 173.

[19] J. Roth, in: R. Behrisch (Ed.), Sputtering at Particle Bombardment II, Springer, Berlin, 1983.

[20] W. Eckstein, C. García-Rosales, J. Roth, W. Ottenberger Sputtering Data, Max-Planck-Institut für Plasmaphysik, Report IPP 9/92, 1993.

[21] H.L. Bay, J. Roth, J. Bohdansky, J. Appl. Phys. 48 (1977) 4722.

[22] M. Balden, J. Roth, J. Nucl. Mater. 280 (2000) in press.

[23] J. Roth, J. Nucl. Mater. 266–269 (1999) 51.

[24] J. Roth, C. García-Rosales, Nucl. Fusion 36 (1996) 1647.

[25] J. Roth, C. García-Rosales, Corrig. Nucl. Fusion 37 (1997) 897.

[26] C. Garcia-Rosules, W. Eckstein, J. Roth, J. Nucl. Mater. 218 (1994) 8.

[27] M. Balden, S. Picarle, J. Roth, in: Proceedings of the 14th International Conference on Plasma Surface Interactions, Rosenheim, Germany, May 2000, to be published in J. Nucl. Mater. (2001).